IEEE Transactions on Nuclear Science, Vol. NS-28, No. 3, June 1981

RADIATION HEATING FROM BEAM LOSS ON ISABELLE EJECTION SEPTA*

Alan J. Stevens
Brookhaven National Laboratory
Upton, New York 11973

Abstract

It is anticipated that radiation heating due to beam loss may place severe constraints on the operation of high energy accelerators which utilize superconducting magnets. Losses on ejection septa, assuming an unbunched beam mode of operation, are unavoidable and have direct impact on the design of the extraction system. Calculations of energy deposition densities downstream of ISABELLE ejection septa have been made using a modified version of the hadron cascade Monte Carlo computer program CASIM.[1] The results of these calculations are described, giving emphasis to understanding the physical processes which dominate the energy deposition as a function of lattice geometry, which may include the presence of collimators. It is found that fast forward protons are particularly troublesome, since they are focused by the lattice until a dispersive element is reached. At 400 GeV/c, these leading particles produce an energy density of $\sim 5 \times 10^{-5}$ GeV/(cm^{3}p) in the coils of ISABELLE dipoles, which implies that septum losses be less than 0.1% of the circulating beam if quenches are to be avoided.

Introduction

Superconducting magnets can be quenched by beam loss during the operation of high energy accelerators. Although many sources of beam loss can, in principle, be controlled (e.g. by slow scraping) during accelerator operation, losses on ejection septa, assuming an unbunched beam mode of operation, are unavoidable and have a direct impact on the design parameters of the extraction system. At ISABELLE, two ejection schemes are currently being considered.[2] Among the factors which influence the choice between these two possibilities is the problem of radiation heating of the magnets downsteam of the septa. It is expected that $\lesssim$ 0.1% of the circulating beam ($\lesssim 6 \times 10^{11}$ protons) will interact in the ejection septum, and the secondaries from these interactions may be sufficient to quench downstream magnets. This problem was first addressed in 1975 in a very crude manner.[3] This note summarizes a series of recent calculations which represent a considerable improvement over the early calculations.

Geometry of the Calculation

A highly schematic representation of that portion of the beam line relevant to the calculations presented here is shown in Fig. 1. In one ejection scenario, the first of a series of septum magnets begins $\sim$ 1 m downstream of the upstream Q4, as shown. The alternative scheme has the first septum located immediately downstream of the upstream Q1. These possibilities will henceforth be referred to as the "Q4" and "Q1" geometries. Figure 2 shows a vertical projection of the first (thin) septum. In both the Q1 and Q4 schemes, the first septum is assumed to be 0.25 mm thick aluminum, 3.5 m long. The leading edge displacement from the beam center line (ΔY in Fig. 2) is -1.7 cm (-1.3 cm) in the Q1 (Q4) geometry. The septum is tilted (parallel to the beam) by +0.5 mrad (0.138 mrad) in the Q1 (Q4) geometry. In these calculations (further elucidated in the next section) the extraction channel (not shown in Fig. 1) is treated as a "brick wall", in that all secondaries emerging from the septum whose vertical position and whose divergence is less than the septum tilt (θ in Fig. 2) are assumed to be either transported in the extraction channel or absorbed by the additional (thicker) septa immediately downstream of the initial thin septum. This is shown schematically by the shaded region in Fig. 2. Because of the thickness and orientation of the additional septa, several absorption lengths of material are seen by such secondaries, so that the "brick wall" approximation should be a good one.

The vacuum pipe is assumed to be steel at $4.4 \leq R \leq 4.6$ cm. The approximation of an ISABELLE magnet is shown in Fig. 3. Ideal dipole and quadrupole fields are assumed for R < 5.5 cm. The effects of magnetic field are ignored in the coil and yoke regions which has been shown to be a good approximation in previous calculations.

Protective steel collars, one meter long and extending between 4.6 cm < R < 10 cm ("protecting" the coil but outside the vacuum pipe) are assumed in front of each doublet and the first dipole. It turns out, however, that these collars offer little protection because secondaries which dominate the radiation heating are interior to the vacuum pipe. Two sets of calculations have been made. The first set, called "unprotected", corresponds to the geometry as thus far described. In the second set, called "protected", steel jaws (horizontal and vertical) are assumed to be present interior to the vacuum chamber. One set of jaws is assumed to be located one meter downstream of the downstream Q2, since this is the position of a proposed limiting aperture beam scraping collimator. Another set is assumed to be between the septum and the first downstream quadrupole, 10 meters ahead of the latter. In the Q4 geometry, a third set of jaws is assumed 10 m downstream of the upstream Q1. Each pair of jaws is assumed to be one meter of steel. Unsurprisingly, as one closes the opening between the jaws to zero, the protection becomes very good indeed. One must clearly make some assumption as to how far the jaws can be closed down in practice. It has been assumed in this note that the jaws can be closed to within $\pm$ 1.5 cm of the beam centerline (at 400 GeV) in the horizontal direction. In the vertical direction, one must allow for the displacement of the beam during the rise of the ejection kicker. This results in an asymmetric vertical opening which is different for each set of vertical jaws. Typically, an additional opening of $\sim$ 1 cm is required for one or the other of a vertical pair.

Method of Calculation

Secondaries emerging from interactions in the thin septum were created and transported by a modified version of the hadron cascade Monte Carlo computer program CASIM.[1,4] The results obtained are deposited energy per cm^3 per interacting proton in the coils of the magnets. Calculations were done only at 400 GeV where the enthalpy reserve of the superconducting magnets is lowest.

A total of 16 calculations were made.* Both geometries, Q1 and Q4, were considered in both the unprotected and protected versions. For each of these 4 geometries, an unbiased and biased calculation was made. This is necessary to obtain reasonable statistical accuracy for the dipoles, which are very far away from the primary interaction. Based on unbiased calculations, it was found that first generation hadrons which lead to energy deposition in the dipoles always

*Work performed under the auspices of the U.S. Department of Energy.

*Some additional calculations were made in the Q4 geometry to test the sensitivity of the small (0.138 mrad) septum tilt on the results. No difference, within statistics, was seen for zero tilt.

0018-9499/81/0600-2924$00.75©1981 IEEE

had energy greater than 250 GeV. Biased calculations were therefore made selecting only first generation hadrons with E > 250 GeV. Finally, for each case discussed, two runs were made with different random number seeds. This made possible an estimate, albeit a somewhat crude one, of a statistical error.

The geometry of the calculation has no symmetry: a vertical asymmetry results from the vertically off-axis source (the septum), and a horizontal asymmetry from the charge asymmetry of the secondaries. For this reason it was necessary to obtain energy deposition as a function of azimuth. The azimuthal angle ϕ is defined in Fig. 3. An x,y scatter plot of points of high energy deposition determined that an appropriate bin width for the azimuthal variable would be $\Delta\phi = 30^{\circ}$. Results are presented in the next section for energy deposition densities for the first 6 mm (6.5 < R < 7.1 cm) of coil. The z (coordinate along the magnet) bin width was defined by subdividing each magnet into either 4 or 5 equal regions.

Results of the Calculation

In all calculations the history of the cascade was traced from the point of interaction in the septum to energy deposition in the magnet coils. This allowed an understanding of which particular processes dominate the energy deposition in each case.

The open symbols in Fig. 4 show the energy deposition density averaged over both z and ϕ for the magnets downstream of the septum in the Q4 geometry. In the unprotected case, the quadrupole magnet nearest the septum suffers the highest energy deposition, as is naively expected. This energy deposition is dominated by second generation charged secondaries which are created by first generation secondaries interacting in the vacuum pipe upstream of this quadrupole. When protective jaws are imposed, the highest energy density occurs in the second quadrupole and is caused primarily by first generation secondaries emerging from the septum itself and second generation secondaries emerging from the faces of the jaws. In both protected and unprotected geometries, energy deposition in the dipoles is dominated by first generation fast forward protons.

Also shown in Fig. 4 (solid symbols) are the maximum energy depositions obtained for the two geometries. In the case of the unprotected quadrupole, the enhancement (relative to the average energy density) occurs at $\phi \sim 90^{\circ}$ and is caused by the vertically defocusing Q2 deflecting primarily positive, soft secondaries into its own coil region. A corresponding enhancement at 270° does not occur because the "brick-wall" approximation of the extraction channel discussed above depletes the $dy/dz < 0$ population. In the protected geometry, quadrupole deposition is dominated by forward positives which are defocused by the upstream Q2 onto the coils of the upstream Q1, again causing a $\phi \sim 90^{\circ}$ enhancement. In the case of the dipoles, a large azimuthal dependence is caused by the fact that, as mentioned above, the deposition is dominated by fast forward (leading particle effect) protons. These protons become dispersed when the dipole fields are encountered and end up highly concentrated on the downstream end and machine-center side ($\phi = 0$) of the second dipole. An azimuthal enhancement of the energy density at $\phi \approx 180^{\circ}$ at the beginning of the second dipole caused by forward neutrals is also observed, but is lower than the values shown in Fig. 4 by a factor of ~ 4.

Results for the Q1 geometry are shown in Fig. 5. Comparison with the Q4 geometry results reveals that the energy deposition densitites in the quadrupoles are less in the Q1 geometry, which is to be expected because the first quadrupoles are farther away from the septum in this case. The energy deposition in the second dipole is, however, the same (within errors) in the two geometries because the dominant component results from leading protons which are focused by the lattice (i.e. whose flux density is not falling like $1/r^2$).

Discussion

It can easily be shown that the fraction of continuous beam lost on a septum of width s is given by $(\tau/T) \cdot (s/d)$ where T is the period of revolution, τ is the rise time of the kicker, and d is the displacement of the central orbit achieved by the kick at the front edge of the septum. The purpose of the foregoing calculations was to define a $\tau \cdot s$ product* such that magnets downstream of the septum will not quench upon routine extraction of the beam. Unfortunately, two large uncertainties make such a definition difficult to achieve. The first of these is the systematic uncertainty associated with the energy deposition calculations described herein. The large distances involved in these calculations makes the results sensitive to possible inadequacies in the particle production model used in CASIM, making these results uncertain by perhaps an order of magnitude.[5] The second uncertainty is the enthalpy limit for ISABELLE magnets. Estimates of this quantity at 400 GeV range from 1.3 mJ/cc to ~ 4 mJ/cc for dipoles, with quadrupoles being a factor of ~ 2 higher.*

Although the absolute error of the calculation might be large, relative errors (Q1 geometry relative to Q4) should be more modest. Table I compares these geometries in terms of the number of protons lost on the septum at the quench limit. This table and the preceeding discussion of the nature of the radiation field allow the following conclusions to be drawn:
1) The concept that long straight sections offer some degree of quench protection, i.e. that secondary energy flux falls off as $1/r^2$, is valid for quadrupoles.
2) This concept is not valid for dipoles. In general, some scheme like the FNAL one, where "dog-legs" with nonsuperconducting dipoles are envisaged, is necessary to reduce the radiation field to a very small value.
3) It may be difficult not to quench one or more ISABELLE magnets during extraction at 400 GeV assuming a continuous beam mode of operation.

Table I. Comparison of Q4, Q1 Geometries

Geometry	Worst Case Quadrupole	Worst Case Dipole
Q4 (unprotected)	1.0	1.3
Q4 (protected)	2.4	9.4
Q1 (unprotected)	3.9	1.9
Q1 (protected)	20.0	11.7

Entries are the number of interacting protons required to quench the indicated magnet x 10^{11} assuming enthalpy limits of 1.5 mJ/cc for dipoles and 3.0 mJ/cc for quadrupoles. Statistical errors are nominally better than a factor of 2.

*As mentioned in the introduction, the $\tau \cdot s$ product currently considered practicable corresponds to a beam loss of $\leq 0.1\%$.

**The quadrupoles have a lower peak field than the dipoles. The uncertainties stem from inexact knowledge of the heat capacity of an ISABELLE braid.

References

1. A. VanGinneken, FNAL-FN-272 (1975).
2. Dr. H. Foelsche, private communication.
3. J. Ranft, et al., Caloric Deposition Downstream of the ISABELLE Beam Scrapers, BNL 20550, 1975 (unpublished).
4. A. VanGinneken, FNAL-FN-309 (1978).
5. A. VanGinneken, private communication.

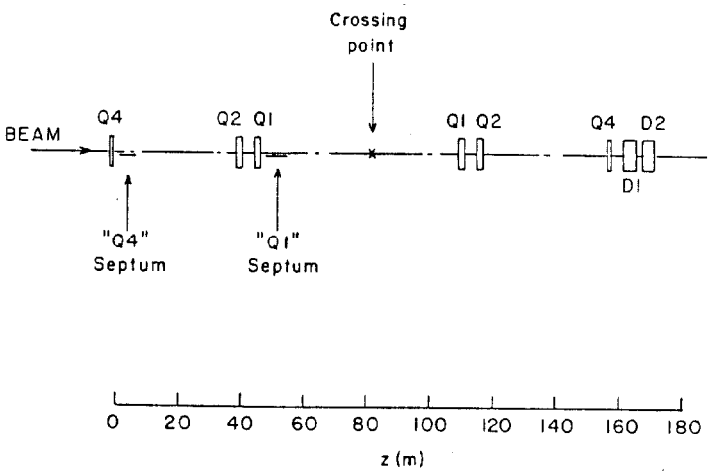

Fig. 1

Fig. 1. Schematic representation of the geometry of the calculation.

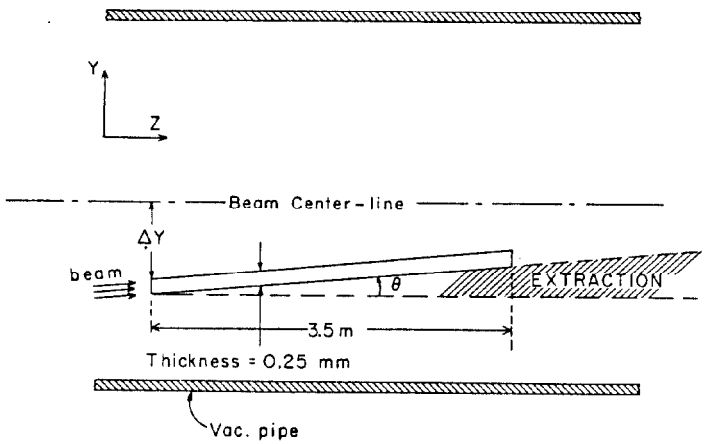

Fig. 2

Fig. 2. Septum detail (not to scale).

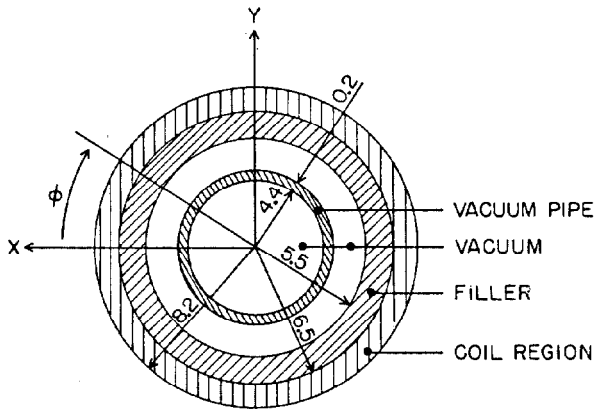

Fig. 3

Fig. 3. Simplified model of an ISABELLE magnet. The coordinate system is such that ring center is toward positive x.

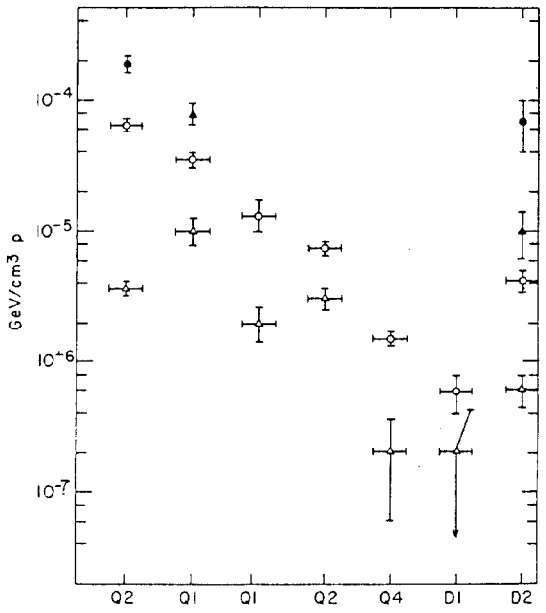

Fig. 4

Fig. 4. Energy deposition densities in the Q4 geometry. The open circles (triangles) give the energy densities averaged over the magnet length and azimuth for the unprotected (protected) calculation. The solid circles (triangles) are the values of maximum energy deposition for the unprotected (protected) calculation.

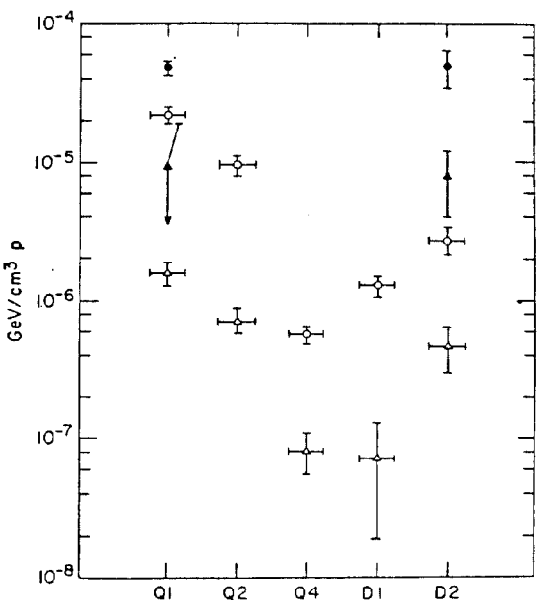

Fig. 5

Fig. 5. As in Fig. 4 for the Q1 geometry.